

An X-Ray Diffraction and Raman Study of Mercury(II) Chloride Complexes in Aqueous Solution. Evidence for the Formation of Polynuclear Complexes

MAGNUS SANDSTRÖM

Department of Inorganic Chemistry, Royal Institute of Technology, S-100 44 Stockholm 70, Sweden

For concentrated mercury(II) chloride solutions ($C_{\text{Hg}} \geq 1$ M), containing a large excess of chloride (mol ratios Cl/Hg ≥ 4.5), the data are consistent with a dominant tetrahedral HgCl_4^{2-} complex with an Hg–Cl bond length of 2.47(1) Å. The vibration frequency $\nu_1(\text{HgCl}_3^-)$ is found to be 288 ± 2 cm^{-1} .

For solutions with Cl/Hg mol ratios around three and $C_{\text{Hg}} \geq 0.5$ M polynuclear complexes occur, probably with distorted octahedral coordination and with double chlorine bridges between the mercury atoms. Structural models for these complexes consistent with the experimental data are proposed.

Dilute aqueous solutions of mercury(II) chloride complexes, which have been investigated by a variety of methods,^{1–3} do not seem to contain polynuclear complexes in detectable amounts. A number of suggestions of polynuclearity³ has not been supported by later careful studies.^{1,4}

The distribution of chloride complexes, HgCl_n^{2-n} ($n=0, 1, 2, 3$, and 4), calculated with the use of equilibrium constants determined by emf methods in 0.5 M (Na)ClO₄ medium,⁵ is given in Fig. 1.

However, in more concentrated solutions polynuclear complexes could occur.³ The solubility of HgCl_2 increases rapidly as the temperature is raised – it is 0.265 M at 25 °C⁶ and 1.81 M at 100 °C.⁷ From an ebullioscopic investigation it was proposed that for concentrations higher than 0.5 M the dominant complex, beside the monomeric HgCl_2 , is the trimeric Hg_3Cl_6 .⁸

Structure of the complexes in solution. An 0.23 M aqueous solution of HgCl_2 was studied by

X-ray diffraction in this work, but no accurate structure information of the complex could be obtained, since the relatively small effects are obscured by the water structure.

There is still some ambiguity of the structure of the HgCl_3^- complex in solution. Incomplete spectra have been reported for several organic solvents^{9–12, 44} and for a melt.¹³ It has not been possible to distinguish between the pyramidal C_{3v} or the planar D_{3h} symmetries on the basis of these spectra. Moreover, the possible coordination of a solvent molecule probably determines which structure the HgX_3^- complex assumes in different solvents.⁹

Pyramidal structures with C_{3v} symmetry have been found for the HgI_3^- and HgBr_3^- complexes in aqueous¹⁴ and DMSO^{15,16} solutions by X-

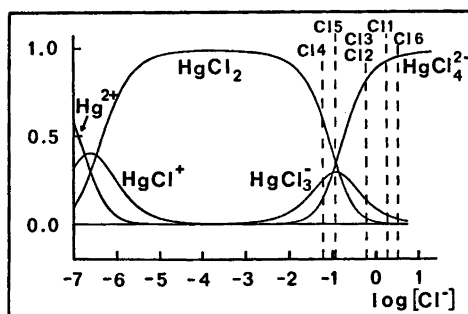


Fig. 1. Fraction of Hg bonded in the different chloride complexes as a function of the free chloride ion concentration. The calculated complex distributions of the solutions investigated by X-ray diffraction, assuming the equilibrium constants to be valid, are indicated.

ray diffraction. Preliminary results of X-ray and Raman studies of 1 M NaHgCl₃ in DMSO solution show that polynuclear complexes are not formed in any large amount.¹⁶ The bond length, 2.44 Å, found from the sharp Hg–Cl peak in the radial distribution function (RDF) is indicative of a pyramidal structure. Thus, by analogy, HgCl₃[–] probably also has C_{3v} symmetry in aqueous solution.

From X-ray scattering measurements on approximately 1 M aqueous solutions of mercury(II) and sodium chloride van Eck proposed that HgCl₄^{2–} is tetrahedral but highly distorted.¹⁷ He found an Hg–Cl bond length of 2.51 Å.

Raman studies of aqueous HgCl₄^{2–} solutions frequently are reported as a simple one-line spectrum.^{18–21} A complete assignment consistent with a tetrahedral T_d symmetry has been made for the spectra of crystalline [(CH₃)₄N]₂HgCl₄,²² which is isomorphous with the corresponding tetrahedral bromide.²³ An earlier study of HgCl₄^{2–} in a melt¹³ appears to lead to an incorrect assignment.²²

In the crystal structure of the salt (AH)₂HgCl₄·2H₂O (where A is the alkaloid perloine, C₂₀H₁₆N₂O₃) discrete HgCl₄^{2–} groups with an average Hg–Cl bond length of 2.50 Å occur. The slight deviation found from a regular tetrahedral structure is probably due to non-bonded compression.²⁴

EXPERIMENTAL

Dried and weighed amounts of mercury(II) chloride (Mallinckrodt, analytical reagent) and lithium or sodium chloride (Merck, suprapur) were dissolved in distilled water and diluted to a known volume. The compositions of the

Table 1. Compositions at 25 °C in mol l^{–1} of the solutions investigated by X-ray diffraction.

Sol.	Hg	Cl	Li	Na	H ₂ O	Ratio Cl/Hg
C11	1.000	5.83	3.827	–	48.1	5.83
C12	1.000	4.50	2.495	–	49.7	4.50
C13	0.999	4.50	–	2.499	52.7	4.50
C14	1.000	2.80	0.798	–	51.7	2.80
C15	5.000	15.00	5.002	–	35.2	3.00
C16	3.400	17.01	10.21	–	33.8	5.00

solutions investigated by X-ray diffraction are given in Table 1.

The diffracted intensity of MoKα radiation (λ=0.7107 Å) was measured at 25 ± 1 °C from the free surface of the solutions in the same way as described previously.¹⁴

Raman spectra were obtained with a Cary 82 Spectrophotometer using the 4880 Å Ar⁺–Kr⁺ laser excitation. Slit widths corresponded typically to 5 cm^{–1}. The solutions were contained in a quartz capillary.

DATA TREATMENT

The processing of the X-ray data was performed as described before.¹⁴ The additional scattering factors needed for Li(0) and Cl(0) were taken from the same sources as before.¹⁴ The calculated double scattering¹⁴ did not exceed 3 %. All curves are calculated for a stoichiometric unit of volume corresponding to one mercury atom.

Least squares refinements of parameters for intramolecular interactions¹⁴ in the mercury(II) chloride complexes were performed. A minimum was sought for the function $U = \sum_{s(1)}^{s(2)} w(s) [i_{\text{obs}}(s) - i_{\text{calc}}(s)]^2$. Due to the relatively larger influence of intermolecular intensity than in the iodide and bromide solutions,¹⁴ only the outermost parts of the reduced intensity curves, $i_{\text{obs}}(s)$, could be used. The contribution of the intramolecular Cl–Cl interaction is too small, however, to permit its parameters to be independently refined in these intervals.

Two models were used for the refinements: (a) allowing only for the Hg–Cl interaction and (b) a regular tetrahedral HgCl₄^{2–} complex where the temperature coefficient for the Cl–Cl interaction was kept constant at the mean value, $b_{\text{X-X}} = 0.028 \text{ Å}^2$, which was obtained for the HgBr₄^{2–} and HgI₄^{2–} complexes.¹⁴ This corresponds to a root-mean-square variation of 0.24 Å in the distance $r_{\text{Cl-Cl}}$, which can be compared to the mean amplitude of vibration 0.1932 Å, calculated for HgCl₃[–] in TBP solution from spectral data.²⁵ The parameters refined in the models are the distance, $r_{\text{Hg-Cl}}$, the number of Hg–Cl distances per mercury atom, $n_{\text{Hg-Cl}}$, and the temperature coefficient, $b_{\text{Hg-Cl}}$. For the solutions C14 and C15 no least-squares refinement results are given, since they contain mercury chloride complexes with several different Hg–Cl distances.

Table 2. Results of least squares refinements for an Hg-Cl interaction; r is the distance, n the number of distances per mercury atom, and b the temperature coefficient.

Sol.	Interval s_1 to s_2	$r/\text{Å}$	n	$b/\text{Å}^2$
Cl1	8-15	2.469(3)	4.3(3)	0.006(1)
Cl2	8-15	2.454(4)	4.0(4)	0.007(1)
Cl3	8-15	2.436(2)	3.3(2)	0.004(1)
Cl6	6-16	2.469(3)	3.7(3)	0.009(2)

RESULTS

X-Ray data. The addition of the intramolecular Cl-Cl interaction, which is the only difference between the refined models, gave slightly lower error square sums, U . However, no significant differences occurred in the parameter values for the two models (Table 2) in the same s interval. The standard deviations given are the ones calculated in the least squares process for a weighting function, $w(s)$, pro-

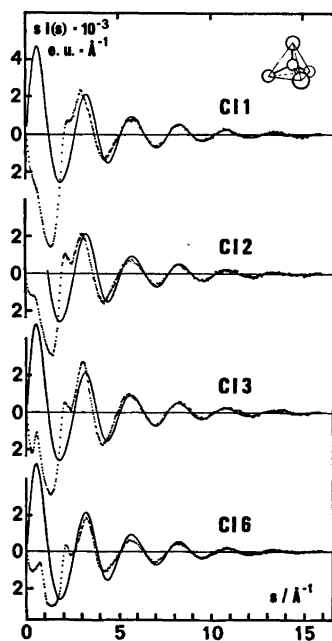


Fig. 2. Reduced intensity values, $i(s)$, multiplied by s , (dots), for the solutions containing an excess of chloride ions. The solid lines give calculated $si(s)$ values for a regular tetrahedral HgCl_4^{2-} complex.

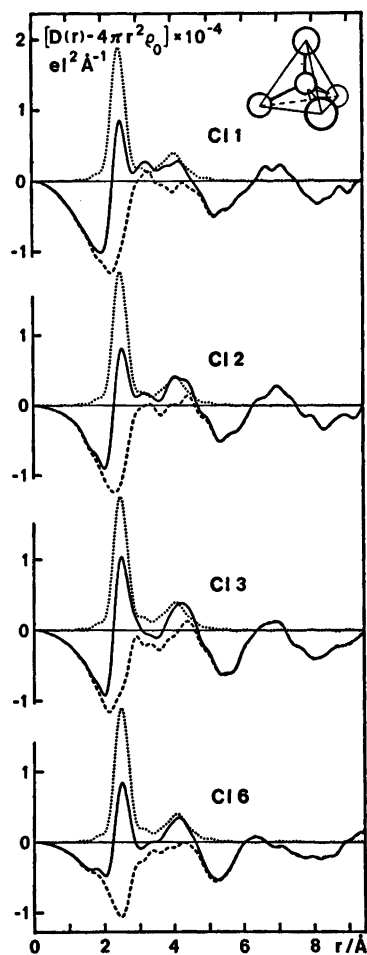


Fig. 3. Experimental $D(r) - 4\pi r^2 \rho_0$ functions for the solutions (solid lines), compared with peak shapes calculated for a regular HgCl_4^{2-} tetrahedron (dotted lines). The difference is shown by the dashed lines.

portional to $\cos \theta / I^2_{\text{corr}}$.¹⁴ The systematic errors seem to be of at least the same order of magnitude as estimated from the variation of the parameter values from refinements in various s intervals.¹⁴

Fig. 2 shows the experimental $si(s)$ curves compared with the calculated curves for a regular HgCl_4^{2-} tetrahedron for the solutions Cl1, Cl2, Cl3, and Cl6. The parameters used are $r_{\text{Hg-Cl}} = 2.47 \text{ Å}$, $b_{\text{Hg-Cl}} = 0.006 \text{ Å}^2$, $n_{\text{Hg-Cl}} = 4$ and $b_{\text{Cl-Cl}} = 0.028 \text{ Å}^2$. The corresponding experimental $D(r) - 4\pi r^2 \rho_0$ functions and the peak

shapes for the HgCl_4^{2-} complex, obtained by Fourier transformation of the intensity curves,¹⁴ are shown in Fig. 3.

In solutions Cl4 and Cl5 (Fig. 7), with mol ratios $\text{Cl}/\text{Hg} \leq 3$, a minor peak at about 2.9 Å is observed in addition to the larger peaks at 2.44 and 2.45 Å, respectively. A large peak at 4.2 Å also occurs for both solutions.

Raman measurements. Two series of solutions were studied. In the first the Cl/Hg mol ratio was varied from 2 to 9, keeping the total mercury concentration, C_{Hg} , at 1 M in most of the solutions. The results are given in Table 3. In the second series the Cl/Hg mol ratio was kept constant at 3.0, while C_{Hg} was varied from 0.050 to 5.00 M. The spectra obtained are shown in Fig. 10.

DISCUSSION

X - Ray data

The peak at 2.4–2.5 Å, corresponding to Hg–Cl distances, is of approximately the same size for the solutions Cl1, Cl2, Cl3, and Cl6, but is smaller in the cases of solutions Cl4 and Cl5, which have much lower Cl/Hg mol ratios. However, the broad peak at 4 to 4.5 Å grows larger as the Cl/Hg mol ratio is reduced.

In the previous study of iodide and bromide complexes¹⁴ Na^+ was the cation. However, in this study Li^+ was used, except for solution Cl3, in order to avoid overlap between the peaks corresponding to the $\text{Na}^+ - \text{H}_2\text{O}$ and Hg–Cl distances.* The difference between the $D(r) - 4\pi r^2 \rho_0$ functions for solutions Cl3 (Na^+) and Cl2 (Li^+), which have the same mercury and chloride concentrations, demonstrates the effects of the strong $\text{Li}^+ - \text{H}_2\text{O}$ coordination²⁶ (Fig. 4). In this difference curve the $\text{Na}^+ - \text{H}_2\text{O}$ interactions give rise to a peak at 2.4 Å. In solution Cl3 the remaining water structure is less disturbed and this appears as broad peaks at about 2.8 and 4.5 Å.²⁷

The Cl– H_2O distances at about 3.1–3.2 Å^{26,28} and O–O distances at about 3.27 Å within a $\text{Li}(\text{H}_2\text{O})_4^+$ tetrahedron,²⁶ can explain the peaks found at about 3.2 Å in solutions Cl1, Cl2 and Cl6. This is demonstrated in Fig. 5, where the hydration model proposed for the

* This overlap probably also affects the parameter values obtained for solution Cl3 in Table 2.

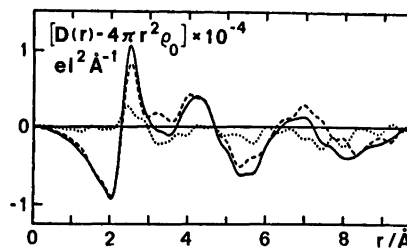


Fig. 4. The difference (dotted line) between $D(r) - 4\pi r^2 \rho_0$ functions for solutions Cl3 (solid line) and Cl2 (dashed line).

HgX_4^{2-} complexes in the preceding article,¹⁴ has been used for solution Cl1 together with independent $\text{Li}(\text{H}_2\text{O})_4^+$ and $\text{Cl}(\text{H}_2\text{O})_6^-$ groups.²⁶ The small amount of free residual water structure was approximately accounted for by assuming a tetrahedral arrangement in $(\text{H}_2\text{O})_6$ units.²⁷ Remaining interactions in the solution were approximated to even electron distributions around these groups.¹⁴ The radii used were 4.95, 3.4, 4.0 and 2.6 Å for the hydrated HgCl_4^{2-} , $\text{Li}(\text{H}_2\text{O})_4^+$, $\text{Cl}(\text{H}_2\text{O})_6^-$ and H_2O species, respectively. A much larger variation in the distances between the HgCl_4^{2-} complex and the water molecules in its surrounding hydration layer had to be assumed than for the bromide and iodide solutions, thus indicating a more irregular hydration sphere. This is probably an effect of the much stronger coordination of water by Li^+ than by Na^+ .²⁶

The described model gives a reasonable account of the experimental intensities and RDF's (Fig. 5). The Hg– H_2O interactions for the hydrated complex give a large and broad peak at about 4.1 Å, which overlaps the intramolecular Cl–Cl interactions. Thus, the direct use of the observed peaks at 4.2 and 4.1 Å in solutions Cl1 and Cl6, respectively, to detect irregularities in the structure of the tetrahedral HgCl_4^{2-} complex is of little value, especially as intramolecular Cl–Cl contacts also can contribute to this peak in the very concentrated solution Cl6. However, the temperature coefficients, $b_{\text{Hg-Cl}}$ (Table 2), are of the same magnitude as found for the HgI_4^{2-} and HgBr_4^{2-} complexes,¹⁴ which indicate all the Hg–Cl bond lengths to be equal. The subtraction of the peak shapes calculated for a regular HgCl_4^{2-} tetrahedron leaves a rather smooth background curve (Fig. 3). A regular tetrahedral

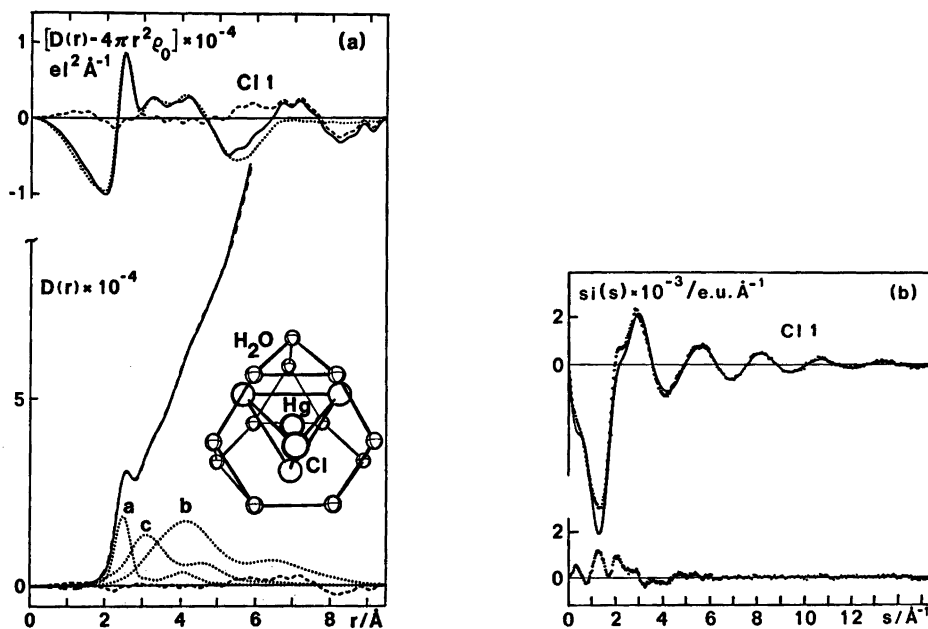


Fig. 5. (a) Comparison between the experimental RDF's for solution Cl1 (solid lines) and the calculated $D(r) - 4\pi r^2 \rho_0$ function (dotted curve) and $D(r)$ curve (long dashes almost coinciding with the solid line), containing both intra- and intermolecular interactions. The difference is shown by the dashed curves. The dotted curve, *a*, shows the peak shapes calculated for an HgCl_4^{2-} tetrahedron, *b* shows the interactions between the HgCl_4^{2-} complex and its surrounding hydration layer and *c* the peak shapes for the interactions within the $\text{Li}(\text{H}_2\text{O})_4^+$ and $\text{Cl}(\text{H}_2\text{O})_6^-$ groups and for the residual water structure. In addition, the calculated $D(r)$ curve contains contributions from the even electron distributions assumed to surround these groups. (b) Comparison between the corresponding experimental (dots) and calculated (solid lines) $si(s)$ curves. The difference is marked by dots below.

structure thus seems to be probable for the HgCl_4^{2-} complex.

Polynuclear complexes. The large peak at about 4.2 Å in solutions Cl4 and Cl5 with mol ratios $\text{Cl}/\text{Hg} \leq 3$ must, because of its size, be due to intramolecular Hg–Hg and Hg–Cl interactions, which means that polynuclear complexes are formed. However, at longer distances no pronounced peaks, indicating distinct intramolecular interactions, are present.

The two distances observed at about 2.4 and 2.9 Å in both solutions correspond approximately to Hg–Cl bond lengths found in crystal structures.^{30–39}

Another indication of polynuclearity is the considerable solubility of mercury dichloride in these almost saturated solutions. If the equilibrium constants used to calculate the distribution of complexes (Fig. 1) are reasonably valid even for these concentrated solutions and

assuming no polynuclear complexes are formed, then the calculated concentrations of the HgCl_2 complex should amount to 0.55 M and 2 M in solutions Cl4 and Cl5, respectively. This greatly exceeds the solubility of HgCl_2 at 25 °C, which is 0.265 M.⁶

Comparisons with crystal structures. In most mercury(II) compounds the mercury atoms are joined by double chlorine bridges. Only in a few adducts of HgCl_2 double oxygen bridges are known to occur.^{36,40} The oxygen atoms then belong to strongly polar groups in the adduct molecules and have a high electron density which favours bridge-formation.^{40,41} In the aqueous solutions studied here, where chloride ions have been added to mercury dichloride, water molecules should not be expected to take part in any bridge formation.

Both distorted tetrahedral^{24,37–40} and distorted octahedral^{30–37,42–44} coordination around

mercury, have been observed in crystal structures. Tetrahedral coordination with double chloride bridges, which has been found in a few discrete dimeric complexes,³⁸⁻³⁹ does not seem to be consistent with the present scattering data since: (a) the Hg-Hg distances at about 3.9 Å would be too short to explain the observed peaks at 4.2-4.3 Å, (b) the area of the peak shapes calculated for a dimeric complex is too small to account for the large peaks observed and (c) this type of coordination seems to occur only when some of the non-bridging ligands are bulky.

A single chloride bridge between four-coordinated mercury atoms is found in very few compounds.^{22,27,44} In single-bridged chains short Hg-Hg distances of suitable length could occur. However, to explain the size of the observed peaks the chains must be rather long, since the average number of Hg-neighbours at about 4.2 Å around each Hg-atom including mononuclear complexes, seems to be approximately 1.5 and 1.8 in solution Cl4 and Cl5, respectively, as is shown in the subsequent calculations. These chains would then have to be rather flexible to account for the absence of pronounced peaks at longer distances in the RDF's.

A more probable structure is the distorted octahedral coordination around mercury, with two short bonds in an approximately linear arrangement which is found, for instance, in a number of complex halides, $MHgCl_3$ and $MHgCl_4$, and in hydrates of these, where M is an alkali or ammonium ion.^{31-35,44} In the crystals the double chloride bridges can be formed both by chlorine atoms in the linear $HgCl_2$ units and by other chloride ions with the $HgCl_2$ units perpendicular to the plane of the bridge (Fig. 6).

The Hg-Cl bond lengths in the linear $HgCl_2$ unit are fairly constant. With few exceptions they fall in the range 2.30 to 2.36 Å. They increase when the donor atoms of the other ligands have a high electron density, especially a negative charge.³⁹

Calculations of peak shapes for the polynuclear complexes. Peak shapes calculated for dinuclear complexes could not entirely account for the 4.2 Å peak in the RDF's of solutions Cl4 and Cl5. The use of a fragment of a double chain structure³⁰ (Fig. 6) to form a triangular trinuclear complex of octahedra with common

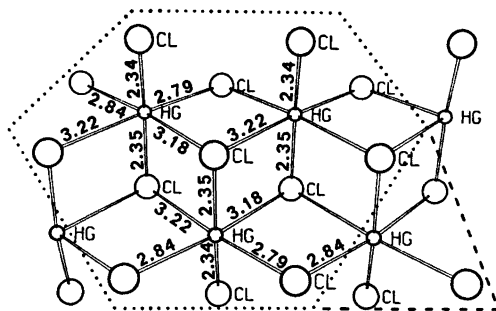


Fig. 6. The double chain, $(HgCl_3^-)_n$, from the crystal structure in Ref. 30. The Hg-Cl bond distances are given in Å. The trinuclear chain fragment used in the calculations for solution Cl4 is outlined by the dotted line, and the tetranuclear fragment used for solution Cl5 is contained within the dotted and dashed lines.

edges, gave a satisfactory agreement with the RDF's and intensity curves for solution Cl4. For solution Cl5 a tetranuclear chain fragment had to be assumed to account for the relatively larger 4.2 Å peak (Figs. 7 and 8). As shown in Fig. 7, complexes of higher nuclearity than three would be expected to give rise to peaks at larger distances in the RDF, where no distinct experimental peaks are found. However, frequent intermolecular interactions in this very concentrated solution (5 M $LiHgCl_3$) could not only obscure such effects but also give substantial contributions to the 4.2 Å peak. This, thus, prevents more definite conclusions about the average nuclearity.

The models used for the final calculations consisted of a trinuclear complex (0.25 M) and a tetranuclear complex (0.9 M) for solutions Cl4 and Cl5, respectively. The remaining amount of mercury, 25 and 28 %, respectively, was assumed to be present in pyramidal $HgCl_3^-$ complexes, with an assumed bond length of 2.45 Å. The peak shapes calculated for these ratios between linear $HgCl_2$ units in the polynuclear complexes and the pyramidal $HgCl_3^-$ complexes were found to reasonably account for the first Hg-Cl peak in the RDF's of the two solutions. The possible occurrence of some $HgCl_4^{2-}$ complexes instead of $HgCl_3^-$ will not affect the results significantly. As before $Li(H_2O)_4^+$ tetrahedra were assumed and for solution Cl4 the contributions from the residual free water structure were approximated by a

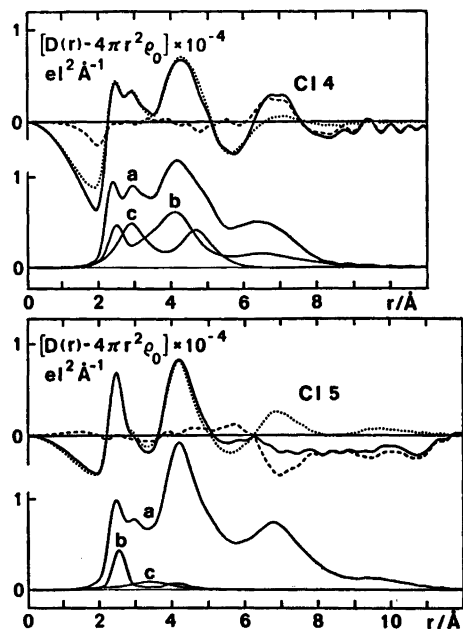


Fig. 7. The experimental $D(r) - 4\pi r^2 \rho_0$ functions (solid lines) for solutions Cl4 and Cl5, compared with the calculated $D(r) - 4\pi r^2 \rho_0$ curves (dotted lines), containing both intra- and intermolecular interactions. The difference is shown by the dashed line. The solid lines below are calculated peak shapes. For solution Cl4 they correspond to: a, the trinuclear complex (Fig. 6) of an average composition $\text{Hg}_3\text{Cl}_{8.3}(\text{H}_2\text{O})_{4.7}$ (0.25 M); b, the HgCl_3^- complex, with its surrounding hydration layer (0.25 M); and c, the $\text{Li}(\text{H}_2\text{O})_4^+$ tetrahedron (0.80 M) plus the residual water structure. For solution Cl5 they are: a, the tetranuclear complex $\text{Hg}_4\text{Cl}_{12}(\text{H}_2\text{O})_3$ (0.9 M); b, the HgCl_3^- complex (1.4 M); and c, the $\text{Li}(\text{H}_2\text{O})_4^+$ tetrahedron (5.0 M).

The calculated $D(r) - 4\pi r^2 \rho_0$ curves also contain contributions from the even electron distribution assumed around the complexes.

tetrahedral arrangement in $(\text{H}_2\text{O})_5$ groups,²⁷ which also gives a contribution to the experimental peak at 2.9 Å. The remaining diffuse interactions in the solutions were approximated as even electron distributions¹⁴ around the assumed complexes and molecules outside radii approximately corresponding to the radii of the species.

In the polynuclear complexes all bridging and linearly coordinated atoms were assumed to be chlorine. The octahedral coordination was completed by the remaining chloride ions and by

water molecules placed about 2.6 Å from the mercury atoms.^{35,46} Stoichiometric considerations then give average compositions for the polynuclear complexes corresponding to $\text{Hg}_3\text{Cl}_{8.3}(\text{H}_2\text{O})_{4.7}$ for solution Cl4 and $\text{Hg}_4\text{Cl}_{12}(\text{H}_2\text{O})_3$ for solution Cl5.

For solutions Cl2 and Cl3 (mol ratios Cl/Hg = 4.5) the peak at 4.2 Å is somewhat larger (Fig. 3) and the Hg-Cl bond length is slightly shorter (Table 2) than for solution Cl1 (mol ratio Cl/Hg = 5.8). These effects indicate that polynuclear complexes, containing roughly 10 to 20 % of the mercury atoms, are still present.

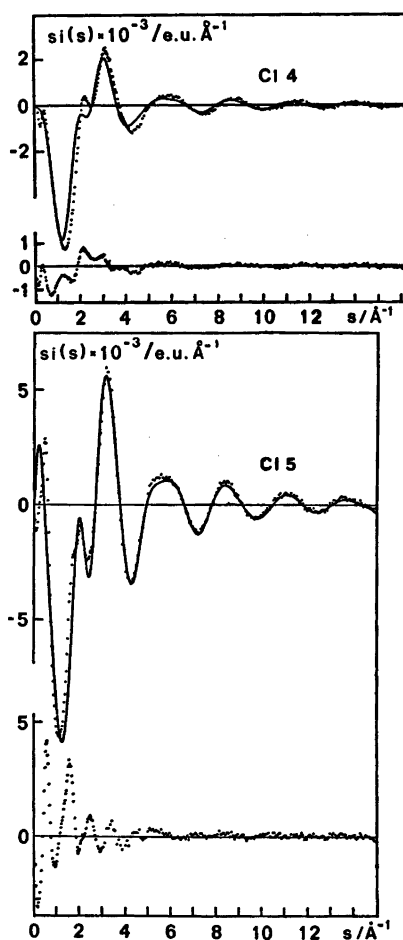


Fig. 8. Comparison between the experimental (dots) and calculated (solid lines) $si(s)$ curves corresponding to the RDF's in Fig. 7. The difference is shown separately underneath (dots).

Table 3. Raman frequencies found for some mercury(II) chloride solutions.

Sol.	C_{Hg}/M	Ratio: Cl to Hg	ν/cm^{-1}	
Cl1	1.00	9.0	270(s)	
	1.00	7.4	270.5(s)	
	1.00	5.83	270(s)	
	Cl6	5.00	5.00	270(vs)
	Cl2	1.00	4.50	270(s)
	Cl3	1.00	4.50	270(s)
Cl4	1.00	3.00	275(s), ~312(m,br)	
	1.00	2.80	~270(w), ~285(m,br), ~312(m,br)	
			~270(vw), ~288(w), 320(m)	
			322(m)	
			0.25	2.80
	0.23	2.00	322(m)	

Raman data

For the first series of solutions where the Cl/Hg mol ratio is varied from 2 to 9, the results in Table 3 show the ν_1 symmetrical stretching frequency to be $270 \pm 1 \text{ cm}^{-1}$ for the HgCl_4^{2-} complex and $322 \pm 1 \text{ cm}^{-1}$ for the HgCl_2 complex in good accordance with previously reported values.^{18-21,47} No other frequencies could be observed in these spectra. The results support the conclusions from the X-ray investigation that the HgCl_4^{2-} complex is dominating in the solutions Cl1, Cl2, Cl3 and Cl6. The presence of a minor amount of polynuclear complexes in solutions Cl2 and Cl3, as indicated by the X-ray data, is supported by the asymmetrical broadening towards higher wave-numbers observed for the Raman bands of these solutions.

For the second series of solutions with constant mol ratio Cl/Hg = 3, the principal shape of the Hg-Cl band should not change if the relative complex distribution remains the same. This would be the case if only mononuclear complexes are formed and the free chloride concentration is negligible. Fig. 9, calculated with the equilibrium constants in Ref. 5, shows that this should be approximately valid at least for concentrations $C_{\text{Hg}} > 0.5 \text{ M}$, but at lower concentrations, where the free Cl^- concentration cannot be neglected, the HgCl_2 complex would dominate.

The spectra of this series (Fig. 10) can be interpreted in the following way. At the lowest

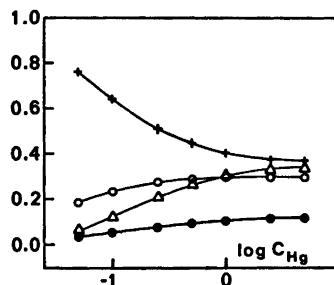


Fig. 9. Relative distribution of mercury(II) chloride complexes at constant mol ratio Cl/Hg = 3, as a function of the total mercury concentration, C_{Hg} . The curve with symbols + gives the ratio $[\text{HgCl}_2]/C_{\text{Hg}}$, the symbol O denotes $[\text{HgCl}_3^-]/C_{\text{Hg}}$, and Δ $[\text{HgCl}_4^{2-}]/C_{\text{Hg}}$. The free chloride ion concentration in mol/l is given by the curve marked with the symbol ●.

concentration studied, $C_{\text{Hg}} = 0.05 \text{ M}$, only the HgCl_2 band at 322 cm^{-1} can be seen. When the concentration is raised, first a band at $288 \pm 2 \text{ cm}^{-1}$ assigned to $\nu_1(\text{HgCl}_3^-)$ and then the band $\nu_1(\text{HgCl}_4^{2-})$ at 270 cm^{-1} start to contribute. No contributions from polynuclear complexes could be detected for concentrations $C_{\text{Hg}} < 0.5 \text{ M}$. At 0.5 M , however, two new bands at 305 ± 3 and $275 \pm 1 \text{ cm}^{-1}$ appear and become dominating at higher concentrations. These frequencies must arise from the polynuclear complexes observed by X-ray diffraction.

Raman and IR studies have been made of crystalline salts, $\beta\text{-NH}_2\text{HgCl}_2$ and $\beta\text{-ND}_4\text{HgCl}_2$, with the double chain structure (Fig. 6) proposed for the polynuclear complexes in solution.⁴⁴ Two Raman bands at 297 and 262 cm^{-1} and at 300 and 265 cm^{-1} , respectively, were found. They were assigned to the symmetrical terminating and bridging Hg-Cl frequencies, respectively. That the same assignments can be made for the two new bands observed for concentrated solutions is supported by the measured depolarization ratios $\rho = I_{\parallel}/I_{\perp}$. For the 0.23 M HgCl_2 solution $\rho = 0.14$ was obtained, which is comparable to the values found by Brill for the HgCl_2 complex in other solvents.⁴⁸ Approximately the same ρ -value was found for the band at 305 cm^{-1} , which thus should correspond to the symmetrical stretching frequency of the HgCl_2 unit. The other Hg-Cl frequencies observed have much lower depolarization ratios, which was helpful in determining the position of this band.

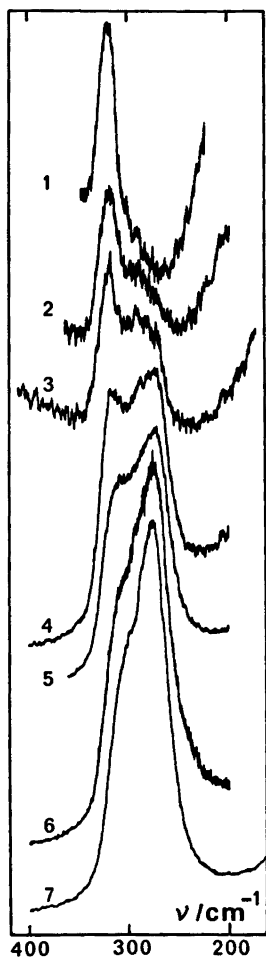


Fig. 10. The Raman bands observed for the series of solutions with constant mol ratio Cl/Hg=3. The total mercury concentrations were 0.050, 0.10, 0.25, 0.50, 1.00, 2.50, and 5.00 M for the solutions 1 to 7, respectively.

The relative intensity scales used for the curves 1 to 7 correspond approximately to the ratios 1:2:4:8:20:40:100, respectively.

CONCLUSIONS

The experimental data are consistent with a regular tetrahedral structure for the HgCl_4^{2-} ion with a bond distance of 2.47(1) Å. It has not been possible to obtain any direct information about the structure of the HgCl_3^- complex in aqueous solution.

In concentrated solutions with $C_{\text{Hg}} \geq 0.5$ M and a Cl/Hg mol ratio around three, polynuclear

complexes occur. The X-ray diffraction data are reasonably well explained by assuming the dominating complex to be tri- or tetranuclear fragments of a double chain structure with double chlorine bridges between the mercury atoms. The coordination around mercury in these complexes is that of a distorted octahedron with two shorter bonds forming a linear unit. Such a model is also compatible with the Raman frequencies observed.

Note added in proof. The crystal structure of Cs_2HgCl_6 contains distorted tetrahedral HgCl_4^{2-} ions, with an average bond length of 2.464 Å.⁴⁰

Acknowledgements. The author is greatly indebted to Dr. G. Johansson for his continuous interest in the work and many helpful suggestions and comments on the manuscript. I also wish to thank Professor K. Larsson for kindly putting the Laser Raman Spectrophotometer at my disposal and Mr. I. Duncan for linguistic help. This work has been supported by the Swedish Natural Science Research Council. Computer time was made available by the Computer Division of the National Swedish Office for Administrative Rationalization and Economy.

REFERENCES

1. Sillén, L. G. and Martell, A. E. *Stability Constants*, Spec. Publ. No. 17 (1964) and *Suppl. No. 1*, Spec. Publ. No. 25, The Chemical Society, London 1971.
2. Deacon, G. B. *Rev. Pure Appl. Chem.* 13 (1963) 189.
3. *Gmelin Handb. Anorg. Chem.* Hg-B2, Verlag Chemie, Weinheim/Bergstr. 1967.
4. Ciavatta, L. and Grimaldi, M. *J. Inorg. Nucl. Chem.* 30 (1968) 197.
5. Lindgren, B., Jonsson, A. and Sillén, L. G. *Acta Chem. Scand.* 1 (1947) 479.
6. Marcus, Y. *Acta Chem. Scand.* 11 (1957) 329.
7. Linke, W. F. *Solubilities of Inorganic and Metal-Organic Compounds*, Van Nostrand, New York 1958.
8. Bourion, F. and Royer, E. *Ann. Chim. (Paris)* 10 (1928) 263.
9. Waters, D. N., Short, E. L., Tharwat, M. and Morris, D. F. C. *J. Mol. Struct.* 17 (1973) 389.
10. Kecki, Z. *Spectrochim. Acta* 18 (1962) 1165.
11. Hooper, M. A. and James, D. W. *Aust. J. Chem.* 24 (1971) 1331 and 1345.
12. Reedijk, J. and Groeneveld, W. L. *Recl. Trav. Chim. Pays-Bas* 88 (1969) 655.
13. Janz, G. J. and James, D. W. *J. Chem. Phys.* 38 (1963) 905.
14. Sandström, M. and Johansson, G. *Acta Chem. Scand. A* 31 (1977) 132.

15. Gaizer, F. and Johansson, G. *Acta Chem. Scand.* 22 (1968) 3013.
16. Sandström, M. *To be published.*
17. van Panthaleon van Eck, C. L. *Thesis*, Leiden 1958, see also Ref. 3.
18. Rolfe, J. A., Sheppard, D. E. and Woodward, L. A. *Trans. Faraday Soc.* 50 (1954) 1275.
19. Davies, J. E. D. and Long, D. A. *J. Chem. Soc. A* (1968) 2564.
20. Delwaille, M.-L. *Bull. Soc. Chim. Fr.* (1955) 1294.
21. Saraf, J. R., Aggarwal, R. C. and Prasad, J. *Bull. Chem. Soc. Jpn.* 43 (1970) 264.
22. Herlinger, A. W. *Spectrosc. Lett.* 8 (1975) 787.
23. Kamenar, B. and Nagl, A. *Acta Crystallogr. B* 32 (1976) 1414.
24. Ferguson, G., Jeffreys, J. A. D. and Sim, G. A. *J. Chem. Soc. B* (1966) 454.
25. Sanyal, N. K., Goel, R. K. and Pandey, A. N. *Indian J. Phys.* 49 (1975) 546.
26. Narten, A. H., Vaslow, F. and Levy, H. A. *J. Chem. Phys.* 58 (1973) 5017.
27. Narten, A. H., Danford, M. D. and Levy, H. A. *Discuss. Faraday Soc.* 43 (1967) 97, see also Luck, W., Ed., *Structure of Water and Aqueous Solutions*, Verlag Chemie, Weinheim/Bergstr. 1974.
28. Licheri, G., Piccaluga, G. and Pinna, G. *J. Chem. Phys.* 64 (1976) 2437.
29. Kavanau, J. L. *Water and Solute-Water Interactions*, Holden Day, San Francisco 1964.
30. Authier-Martin, M. and Beauchamp, A. L. *Can. J. Chem.* 53 (1975) 2345.
31. Zvonkova, Z. V., Samodurova, V. V. and Vorontsova, L. G. *Dokl. Akad. Nauk SSSR* 102 (1955) 1115.
32. Sagisawa, K., Kitahama, K., Kiriya, H. and Kiriya, R. *Acta Crystallogr. B* 30 (1974) 1603.
33. Malčić S. S. *Bull. Inst. Nucl. Sci. Boris Kidrič* 9 (1959) 115.
34. Harmsen, E. J. *Z. Kristallogr.* 100 (1938) 208.
35. Brusset, H. and Madaule-Aubry, F. *Bull. Soc. Chim. Fr.* 10 (1966) 3122.
36. Biscarini, P., Fusina, L., Nivellini, G. D., Mangia, A. and Pelizzi, G. *J. Chem. Soc. Dalton Trans.* (1973) 159; (1974) 1846.
37. Brotherton, P. D. and White, A. H. *J. Chem. Soc. Dalton Trans.* (1974) 2698.
38. Glasser, D., Ingram, L., King, M. G. and McQuillan, G. P. *J. Chem. Soc. A* (1969) 2501.
39. Brotherton, P. D., Epstein, J. M., White, A. H. and Willis, A. C. *J. Chem. Soc. Dalton Trans.* (1974) 2341.
40. Brändén, C. I. *Ark. Kemi*, 22 (1964) 501.
41. Lindqvist, I. *Inorganic Adduct Molecules of Oxo-Compounds*, Springer, Berlin 1963.
42. Grdenić, D. *Arh. Kem.* 22 (1950) 14.
43. Grdenić, D. and Krstanović, I. *Arh. Kem.* 27 (1955) 143.
44. Barr, R. M. and Goldstein, M. *J. Chem. Soc. Dalton Trans.* (1974) 1180; (1976) 1593; *Inorg. Nucl. Chem. Lett.* 10 (1974) 33.
45. White, J. G. *Acta Crystallogr.* 16 (1963) 397.
46. McPhail, A. T. and Sim, G. A. *Chem. Commun.* 1 (1966) 21.
47. Allen, G. and Warhurst, E. *Trans. Faraday Soc.* 54 (1958) 1786.
48. Brill, T. B. *J. Chem. Phys.* 57 (1972) 1534.
49. Clegg, W., Brown, M. L. and Wilson, L. J. A. *Acta Crystallogr. B* 32 (1976) 2905.

Received August 31, 1976.